Large-Area Highly-Oriented SiC Nanowire Arrays: Synthesis, Raman, and Photoluminescence Properties

Zhenjiang Li,*,† Jinli Zhang,† Alan Meng,‡ and Jianzhang Guo†

College of Electromechanical Engineering and College of Chemistry and Molecular Engineering, Qingdao University of Science and Technology, Qingdao 266061, Shandong, P. R. China

Received: June 8, 2006; In Final Form: September 5, 2006

Large-area highly oriented SiC nanowire arrays have been fabricated by chemical vapor reaction using an ordered nanoporous anodic aluminum oxide (AAO) template and a graphite reaction cell. Their microstructures were characterized by scanning electron microscopy, energy-dispersive X-ray spectroscopy, X-ray diffraction and high-resolution transmission electron microscopy. The results show that the nanowires are single-crystalline β-SiC's with diameters of about 30−60 nm and lengths of about 8 μm, which are parallel to each other, uniformly distributed, highly oriented, and in agreement with the nanopore diameter of the applied AAO template. The nanowire axes lie along the [111] direction and possess a high density of planar defects. Some unique optical properties are found in the Raman spectroscopy and photoluminescence emission from oriented SiC nanowire arrays, which are different from previous observations of SiC materials. The growth mechanism of oriented SiC nanowire arrays is also analyzed and discussed.

Introduction

Recently, there has been increasing interest in oriented nanostructural systems because of their numerous potential applications in optoelectronics, sensors, nanogenerators, and electronic circuits.[1,2] Hierarchical assembly of nanowires in a controlled manner is a critical step toward accomplishing these goals.[3−5] Up to now, much effort has been devoted to the synthesis of one-dimensional oriented nanostructural materials.[6−9] Template-assisted synthesis is an elegant chemical approach for the fabrication of oriented nanostructures, particularly for different solid nanowire arrays. Among these templates, the nanoporous anodic alumina templates have received considerable attention in synthetic nanostructure materials due to their unique structural properties, such as their fully controllable and extremely narrow size distribution in pore diameters, good chemical inertness, physical stability, and ideal cylindrical shape of pores.[10−12] They have been extensively used to fabricate one-dimensional oriented nanomaterials by using a variety of methods.[13−17]

Silicon carbide (SiC) is one of the most promising semiconductors because of its high breakdown electric field (3−5 MV/cm), low coefficient of thermal expansion, and high thermal conductivity (350−490 W m^{-1} K^{-1}), high resistance to oxidation, high hardness, high strength, and low mass density.[18−20] It can be used to fabricate electronic devices operating at high temperature, high power, high frequency, and in harsh environments.[21,22] In addition, SiC one-dimensional nanostructures have displayed unique optical and electron field emission properties,[23−26] especially for oriented SiC nanowire arrays.[27] More recently, many methods to synthesize SiC nanowires (nanorods) have been developed. These methods roughly fall into the following three categories: (1) utilizing a vapor−liquid−solid growth mechanism;[28−30] (2) using a carbon nanotube-confined reaction;[27,31,32] (3) using a carbon-thermal reduction.[33−35] In our previous studies, we have successfully synthesized large-scale SiC nanowires[36] and SiC nanowire networks[37] by a chemical vapor reaction method. Herein, we report for the first time the synthesis of large-area highly oriented SiC nanowire arrays in an ordered nanoporous anodic aluminum oxide (AAO) template through a chemical vapor reaction approach. A mixture of milled Si and SiO_2 powder and C_3H_6 were chosen as the starting materials. Large-area highly oriented SiC nanowire arrays were fabricated in the nanopores of an AAO template via a series of chemical reactions of Si, SiO_2, and C_3H_6.

Experimental Section

Fabrication Process of the AAO Template. The AAO template was prepared by a two-step aluminum anodic oxidation process similar to that previously described, to obtain a uniform pore structure.[38] Prior to anodization, the high-purity aluminum thin sheets (99.99%) were annealed at 450 °C for 2 h, rinsed in distilled water, then electropolished to achieve a smooth surface. Subsequently, the aluminum samples were anodized in 0.3 M oxalic acid (40 V, 17 °C, 4−5 h, Al sheet as an anode). The first-step anodized layer was removed by etching in a mixture of phosphoric acid and chromic acid at 60 °C for 8−10 h. During the second step, the samples rinsed in distilled water and oxalic acid were anodized again in 0.3 M oxalic acid (40 V, 16 °C, 7−9 h, Al sheet as an anode). After the second-step anodization, the unwanted aluminum matrix was dissolved in saturated $HgCl_2$ solution at room temperature. Finally, the template was rinsed with distilled water and immersed in 5% phosphoric acid for about 20−40 min at 32 °C to adjust the pore diameter and remove the barrier layer at the bottom of nanoholes.[39]

Synthesis Steps of SiC Nanowire Arrays. First, Si and SiO_2 powder of 99% purity were milled for 48 h. The ball-milling process was carried out in a rolling laboratory ball mill using hardened agate balls and a resin cell. The containment cell was

* Corresponding author. Phone: +86-532-88958602. Fax: +86-532-88956118. E-mail: zjli126@126.com.
† College of Electromechanical Engineering.
‡ College of Chemistry and Molecular Engineering.

10.1021/jp063565b CCC: $33.50
Published on Web 10/21/2006

loaded with several tens of grams of Si or SiO_2 powder together with 2 balls of 20 mm diameter, 5 balls of 12 mm diameter, 20 balls of 7 mm diameter, and 50 balls of 2 mm diameter. Following milling, the as-milled powders were dried at 90 °C for about 24 h in a constant-temperature oven. A 1.2:1 molar mixture of ball-milled Si and SiO_2 was milled and mixed for 30 min in an agate mortar. The $Si-SiO_2$ mixture and AAO template were placed in a graphite reaction cell. The AAO template was situated over the mixture of $Si-SiO_2$, and a piece of carbon cloth was inserted between the template and the mixture of $Si-SiO_2$. Then the graphite reaction cell was placed into a vertical-tube graphite heater furnace. Prior to heating, the system was flushed three times with high-purity argon (Ar) by using a rotary vacuum pump to reduce the concentration of O_2 to a negligible level from the furnace chamber. The temperature of the furnace was increased to 1230 °C from room temperature at a mean rate of 350−400 °C/h. During the heating, the furnace was evacuated at 1000 °C to obtain a gas pressure of 350 Torr. The steady C_3H_6 flow of 8−10 sccm from the bottom of the graphite reaction cell was started and maintained for 3−5 min at 1230 °C under a total gas pressure of 540−650 Torr. Then the temperature of furnace was decreased to 500 °C at a mean rate of 270−300 °C/h. Finally, the power was switched off, and the furnace was allowed to cool to room temperature in an Ar atmosphere.

Characterization. The morphology and elemental analysis of the nanoporous AAO template and the oriented SiC nanowire arrays were characterized by a Hitachi (Tokyo, Japan) S-4200 field-emission scanning electron microscope (FE-SEM) equipped with energy-dispersive X-ray (EDX) spectroscopy. Prior to SEM observation, the samples were sputter-coated with gold under a high vacuum for 2 min to increase their conductivity. The structure of the resulting material was characterized by using a Rigaku (Japan) D/max-3C X-ray diffractometer with Cu Kα radiation at room temperature. Further detailed structural information of the oriented SiC nanowire arrays was obtained by using a Hitachi (Tokyo, Japan) H-8100 transmission electron microscope (TEM), selected-area electron diffraction (SAED), and a high-resolution transmission electron microscope (HRTEM) (JEOL-2010). For TEM observation, the samples were dispersed in alcohol with the aid of ultrasonic agitation for 30 min, and then a drop of solution was dropped onto a copper grid covered by porous carbon. The Raman scattering spectra were measured with a micro-Raman spectrometer (Renishaw 2000) at room temperature. The 514-nm line of an Ar^+ laser was used as the excitation source. Photoluminescence (PL) spectral measurements were performed in a Hitachi F-4500 fluorescence spectrophotometer using a xenon lamp at room temperature.

Results and Discussion

A typical FE-SEM image of the nanoporous AAO template surface is shown in Figure 1a. The image shows the nanopores on the surface with an average pore diameter of about 30−60 nm and a distance among neighboring pores of about 30−50 nm, which are connected to each other to form the nanonetwork. Figure 1b is the FE-SEM image of the cross-section of the nanoporous AAO template, which depicts the AAO template with pores parallel to each other, uniformly distributed, and perpendicular to the surface of the template.

After the reaction, the area of the products is about 1.5 cm^2, and the color of the samples is light blue. Figure 2 shows the characteristic FE-SEM image of oriented SiC nanowire arrays grown with the assistance of an AAO template. It can be clearly seen that the SiC nanowires, with a length of around 8 μm, are parallel to each other, uniformly distributed, and highly oriented. The density of SiC nanowires is about 10^9-10^{10} cm^{-2}. The EDX spectrum (Figure 3a) collected from the AAO template demonstrates the presence of Al and O. The quantitative analysis indicates their atomic ratio of Al and O is approximately 2:3, corresponding to the stoichiometric composition of Al_2O_3. The EDX spectrum (Figure 3b) collected from oriented SiC nanowire arrays growing in the nanoporous AAO template shows that the nanowires are composed of Si, C, O, and Al. O and Al come from the AAO template. The molecular ratio of Si/C of the nanowires calculated from the EDX data is about 1:1, within the experimental error, corresponding to the stoichiometric composition of SiC. The above SEM and EDX results show that large-area highly oriented SiC nanowire arrays were formed in the nanoporous AAO template.

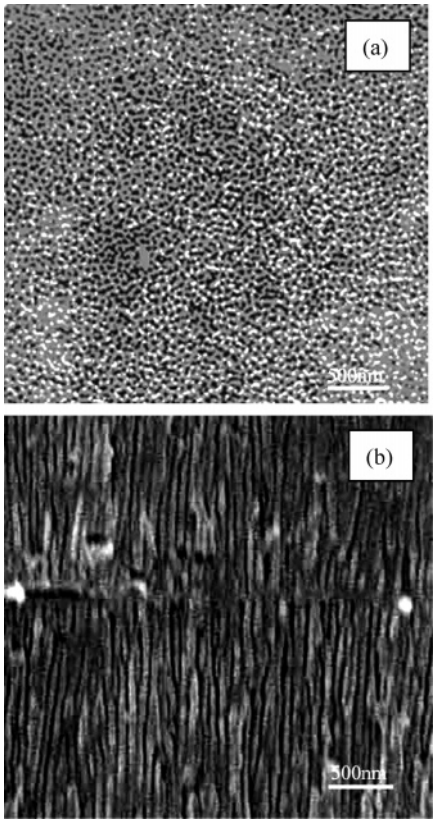

Figure 1. (a) FE-SEM image of the nanoporous AAO template surface. (b) FE-SEM image of the cross-section of the nanoporous AAO template.

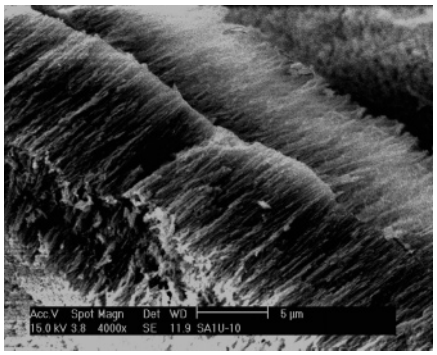

Figure 2. FE-SEM image of oriented SiC nanowire arrays.

A typical X-ray diffraction XRD pattern of oriented SiC nanowire arrays growing in the nanoporous AAO template is shown in Figure 4. The major diffraction peaks are assigned to

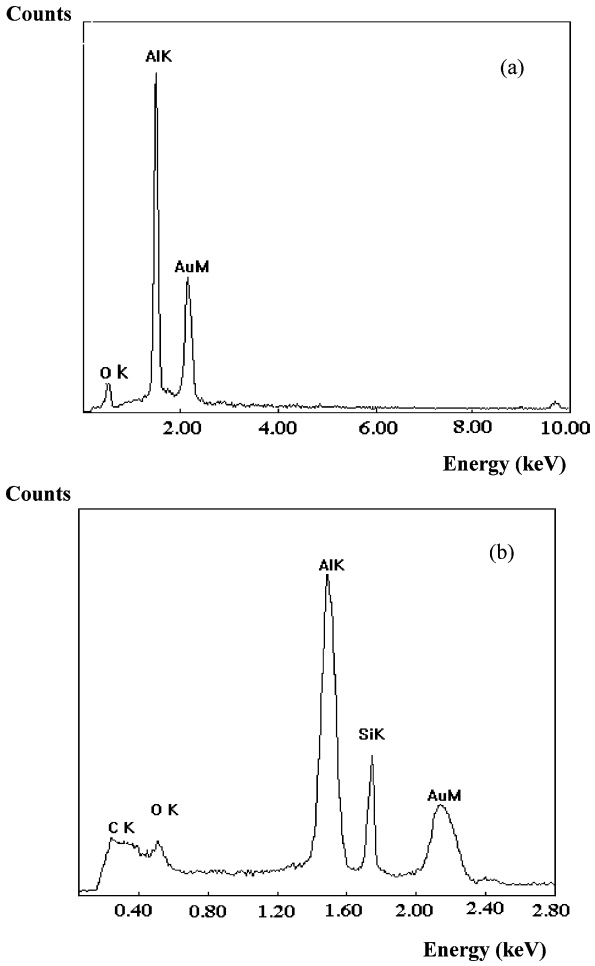

Figure 3. (a) EDX spectrum collected from the AAO template. (b) EDX spectrum collected from oriented SiC nanowire arrays growing in the nanoporous AAO template.

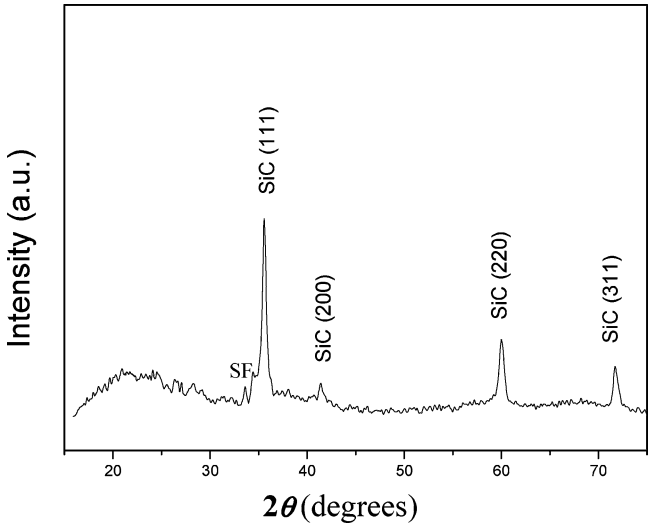

Figure 4. XRD pattern of oriented SiC nanowire arrays.

the (111), (200), (220), and (311) reflections of cubic β-SiC (unit cell parameter $a = 0.4358$ nm). These values are almost identical to the known values for β-SiC (JCPDS Card. No. 29-1129). The peak marked with SF is due to stacking faults. The stronger intensities of β-SiC diffraction peaks (relative to the background amorphous) indicate that the resulting products were well-crystallized β-SiC. In addition, the β-SiC diffraction peaks are obviously broadened, which maybe the result of the effect

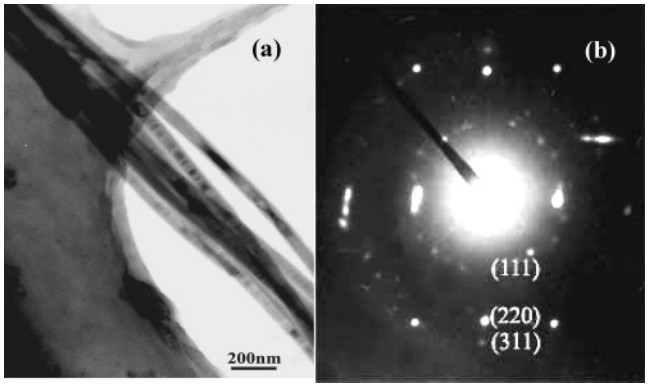

Figure 5. (a) TEM image of oriented SiC nanowires. (b) The corresponding SAED pattern taken from several SiC nanowires.

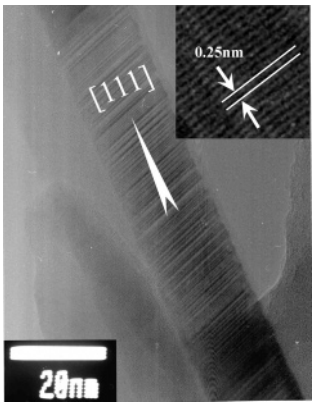

Figure 6. HRTEM image of an oriented SiC nanowire.

of nanosize and surface states, and the diffraction peak bulge between 20° and 25° is the characteristic amorphous Al_2O_3 peak. The above results indicate that large-area highly oriented SiC nanowire arrays have been obtained at relatively low temperatures by a chemical vapor reaction approach.

Figure 5a is a characteristic TEM image of several parallel SiC nanowires, revealing that the periphery of SiC nanowires is very clean, without any wrapping of amorphous material. The diameter of these nanowires is about 30−60 nm, corresponding to the diameter of the nanopores of the AAO template. In addition, we may find that the nanowires are parallel to each other after ultrasonic agitation. The reason is that the SiC nanowires have an oriented arrangement in the AAO template. The corresponding SAED pattern taken from several SiC nanowires is illustrated in Figure 5b. It shows three discrete polycrystalline diffraction rings, which correspond to the (111), (220), and (311) crystallographic planes of cubic β-SiC. Furthermore, the SAED pattern exhibits planar defects and streaks of stacking fault structure. Otherwise, a small number of single-crystal diffraction spots from an individual SiC nanowire suggest a single-crystalline β-SiC structure.

A representative HRTEM image (in Figure 6) depicts steplike streaked lines, which suggest that the SiC nanowires possess a high density of planar defects and stacking faults. We believe that these planar defects occur during the growth process due to thermal stress. The insert in Figure 6 shows that the interplanar spacing, which is perpendicular to the wire axes, is about 0.25 nm, which corresponds to the separation between the (111) lattice planes of β-SiC, suggesting that the axes of the SiC nanowire lie along the [111] direction.

The typical Raman spectra taken from oriented β-SiC nanowires and the AAO template are shown in Figure 7. It indicates that no Raman mode is observed from a bare AAO

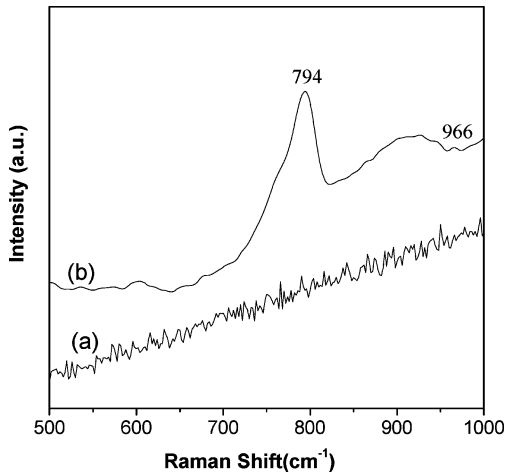

Figure 7. Raman scattering spectra of the AAO template and oriented SiC nanowires. Spectra a and b correspond to the AAO template and oriented SiC nanowires, respectively.

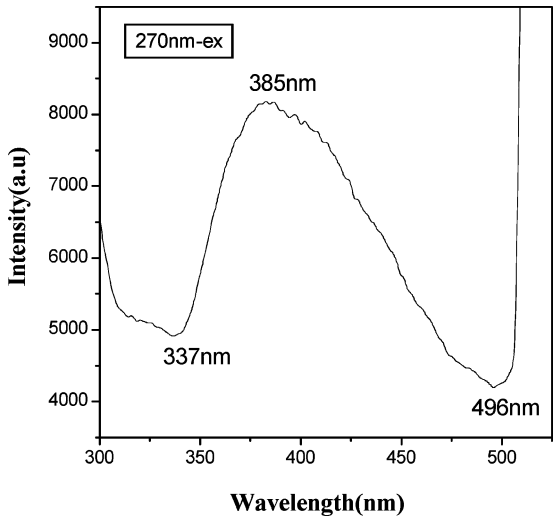

Figure 8. Room-temperature PL spectrum of oriented SiC nanowires.

template (Figure 7a), and there are only two strong peaks at around 794 and 966 cm^{-1} observed, as shown in Figure 7b, corresponding to the TO and LO phonons at the Γ point of cubic SiC. We note that the Raman spectral features are strikingly different from others published elsewhere.[40,41] The TO (Γ) phonon line is not only much stronger than the LO (Γ) phonon line, but both of the lines are also shifted. This difference may be explained by the size confinement effect and stacking faults of oriented β-SiC nanowires.

Figure 8 displays a room-temperature PL spectrum of the β-SiC nanowires. When excited with light from a xenon source (excitation wavelength 270 nm), the nanowires have an emission band between 337 and 496 nm, which is centered at 385 nm. Compared with the previously reported luminescence from the nanospheres,[42] nanowires,[43,44] films,[45] and nanobelts[46] of β-SiC, the emission peak for oriented β-SiC nanowires is obviously shifted to the blue. The reason for these results is yet unknown, and a deeper study on this work is clearly needed.

Although the detailed growth mechanism of oriented SiC nanowire arrays is still not fully understood, the above-mentioned results allow us to suggest a possible process responsible for the formation of the large-area highly oriented SiC nanowire arrays, which is illustrated in Figure 9. The empty AAO template, as shown in Figure 9a, has a number of nanopores with diameters of 30−60 nm before the reactions.

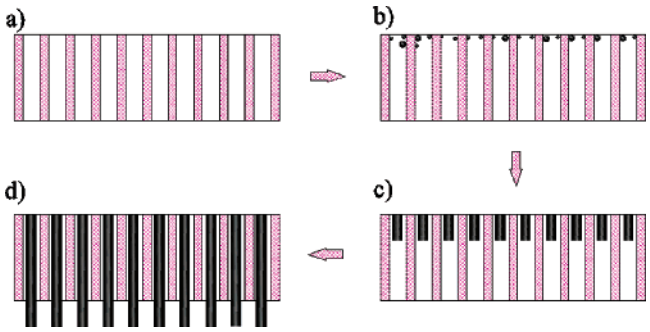

Figure 9. Schematic illustration of the growth process of the highly oriented SiC nanowire arrays growing in the nanoporous AAO template: (a) The AAO template at the beginning of the reaction. (b) Nanosized nucleic SiC deposited on the inside of the pores of the AAO template. (c) The SiC nanowires in the pores are grown along the axial direction. (d) The outside nanowires sustain the axial growth direction of the already formed SiC nanowires in the nanopores of the AAO template.

When the furnace is heated to a high temperature, SiO vapor is generated by a solid−solid reaction between the milled Si and SiO_2; the reaction equation is $Si(s) + SiO_2(s) \rightarrow 2SiO(v)$ (1). Subsequently, C_3H_6 vapor from the bottom of the graphite reaction cell is introduced into the reaction chamber and pyrolyzed C. The capillary effect[47] of the anodic pores with large aspect ratios (depth/diameter) in the AAO template is favorable for the conglomeration of C and SiO vapor in the nanopores and the nucleation of SiC nanowires. When C enters into the pores of the AAO template together with SiO vapor, it quickly reaches the nucleic concentration of the SiC nanowires. Therefore, nanosized nucleic SiC is deposited on the inner surface of the pores of the AAO template (see Figure 9b), by a chemical vapor reaction, which can be expressed as $3SiO(v) + 2C_3H_6(v) \rightarrow 3SiC(s) + 3CO(v) + 6H_2(v)$ (2). For the growth of SiC nanowires, ⟨111⟩ has been demonstrated to be the preferred growth direction, and the growth rate along the ⟨111⟩ axis direction is much faster than that along other directions.[27,48] In addition, the space confinement of the alumina channel is favorable for the ⟨111⟩ axis direction growth of SiC nanowires in the pores of the AAO template (see Figure 9c). When the reactions continue, the subsequently generated SiO and C will react with each other to grow SiC on the top of the formed SiC nanowires because the needed energy growing on the formed SiC nanowire top is far lower than that of nucleic SiC on the other places of the AAO template. So the outside nanowires sustain the axial growth direction of the formed SiC nanowires in the nanopores of the AAO template (see Figure 9d). Withal, we believe that the fabrication of highly oriented SiC nanowire arrays has to decrease the reaction rate and shorten the C_3H_6 reaction time, otherwise the nanosized SiC may be nuclear on the other places of the AAO template simultaneously. In addition, it is very important to put the nanoporous AAO template over the mixture of milled $Si-SiO_2$. To test this, we put the AAO template under the mixture of milled $Si-SiO_2$ to repeat the above process, and no SiC nanowire arrays were found. The reason may be that the oriented flow of the vapor from the bottom of the reaction cell is favorable for driving the C and SiO vapor into the pores of the AAO template and facilitates the oriented growth of SiC nanowires. It should be pointed out that the exact mechanism for the formation of large-area highly oriented SiC nanowire arrays by the presented method should be further investigated, which is now underway with our work.

Conclusion

In summary, large-area highly oriented SiC nanowire arrays have been synthesized by a chemical vapor reaction using an ordered nanoporous AAO template and a graphite reaction cell. SEM, EDX, XRD, and HRTEM investigations on these nanowires have been carried out. The results show that the nanowires are single-crystalline β-SiC's with diameters of about 30−60 nm and lengths of about 8 μm, which are parallel to each other, uniformly distributed, highly oriented, and in agreement with the nanopore diameter of the employed AAO template. The nanowire axes lie along the [111] direction and possess a high density of planar defects. Some unique optical properties are found in the Raman spectroscopy and PL emission from oriented SiC nanowire arrays, which are different from previous observations of SiC materials.

Acknowledgment. This work was financially supported by the National Natural Science Foundation of China under Grant No. 50572041, the Natural Science Foundation of Shandong Province under Grant No. Y2005F08, and also the Science and Technology development plan design of Qingdao City under Grant No. 05-1-GX-06. We express our grateful thanks to them for their support.

References and Notes

(1) Xia, Y.; Yang, P.; Sun, Y.; Wu, Y.; Mayers, B.; Gates, B.; Yin, Y.; Kim, F.; Yan, Y. *Adv. Mater.* **2003**, *15*, 353.
(2) Wang, Z. L.; Song, J. H. *Science* **2006**, *312*, 242.
(3) Whang, D.; Jin, S.; Wu, Y.; Lieber, C. M. *Nano Lett.* **2003**, *3*, 1255.
(4) Melosh, N. A.; Boukai, A.; Diana, F.; Gerardot, B.; Badolato, A.; Petroff, P. M.; Heath, J. R. *Science* **2003**, *300*, 112.
(5) Tao, A.; Kim, F.; Hess, C.; Goldberger, J.; He, R.; Sun, Y.; Xia, Y.; Yang, P. *Nano Lett.* **2003**, *3*, 1229.
(6) Ge, S.; Jiang, K.; Lu, X.; Chen, Y.; Wang, R.; Fan, S. *Adv. Mater.* **2005**, *17*, 56.
(7) Zhang, M.; Lenhert, S.; Wang, M.; Chi, L.; Lu, N.; Fuchs, H.; Ming, N. B. *Adv. Mater.* **2004**, *16*, 409.
(8) Liu, C. H.; Zapien, J. A.; Yao, Y.; Meng, X. M.; Lee, C. S.; Fan, S. S.; Lifshitz, Y.; Lee, S. T. *Adv. Mater.* **2003**, *15*, 838.
(9) He, J. H.; Hsu, J. H.; Wang, C. W.; Lin, H. N.; Chun, L. J.; Wang, Z. L. *J. Phys. Chem. B* **2006**, *110*, 50.
(10) Masuda, H.; Fukuda, K. *Science* **1995**, *268*, 1466.
(11) Che, G.; Lakshmi, B. B.; Fisher, E. R.; Martin, C. R. *Nature (London)* **1998**, *393*, 346.
(12) Miller, S. A.; Young, V. Y.; Martin, C. R. *J. Am. Chem. Soc.* **2001**, *123*, 12335.
(13) Wu, Y. Y.; Livneh, T.; Zhang, Y. X.; Cheng, G. S.; Wang, J. F.; Tang, J.; Moskovits, M.; Stucky, G. D. *Nano Lett.* **2004**, *4*, 2337.
(14) Bogart, T. E.; Dey, S.; Lew, K.-K.; Mohney, S. E.; Redwing, J. M. *Adv. Mater.* **2005**, *17*, 114.
(15) Jeong, S. Y.; Kim, J. Y.; Yang, H. D.; Yoon, B. N.; Choi, S.-H.; Kang, H. K.; Yang, C. W.; Lee, Y. H. *Adv. Mater.* **2003**, *15*, 1172.
(16) Lombardi, I.; Hochbaum, A. I.; Yang, P. D.; Carraro, C.; Maboudian, R. *Chem. Mater.* **2006**, *18*, 988.
(17) Miao, J. Y.; Cai, Y.; Chan, Y. F.; Sheng, P.; Wang, N. *J. Phys. Chem. B* **2006**, *110*, 2080.
(18) Powell, J. A.; Matus, L. G.; Kuczmarski, M. A. *J. Electrochem. Soc.* **1998**, *134*, 1558.
(19) Choyke, W. J.; Pensk, G. *Mater. Res. Soc. Bull.* **1997**, *22*, 25.
(20) Larkin, D. J. *Mater. Res. Soc. Bull.* **1997**, *22*, 36.
(21) Fisher, A.; Schroter, B.; Richter, W. *Appl. Phys. Lett.* **1995**, *66* (23), 3182.
(22) Feng, Z. C.; Mascarenhas, A. J.; Choyke, W. J.; Powell, J. A. *J. Appl. Phys.* **1998**, *64*, 3176.
(23) Wu, Z. S.; Deng, S. Z.; Xu, N. S.; Chen, J.; Zhou, J.; Chen, J. *Appl. Phys. Lett.* **2002**, *80*, 3829.
(24) Zhou, X. T.; Lai, H. L.; Peng, H. Y.; Frederick, C. K. A.; Liao, L. S.; Wang, N.; Bello, I. *Chem. Phys. Lett.* **2000**, *318*, 58.
(25) Zhou, X. T.; Wang, N.; Frederick, C. K. A.; Lai, H. L.; Peng, H. Y.; Bello, I.; Lee, C. S.; Lee, S. T. *Mater. Sci. Eng., A* **2000**, *286*, 119.
(26) Lai, H. L.; Wong, N. B.; Zhou, X. T.; Peng, H. Y.; Au, F. C. K.; Wang, N.; Bello, I.; Lee, C. S.; Lee, S. T.; Duan, X. F. *Appl. Phys. Lett.* **2000**, *76*, 294.
(27) Pan, Z. W.; Lai, H. L.; Frederick, C. K. A.; Duan, X. F., Zhou, W.; Shi, W. S.; Wang, N.; Lee, C. S.; Wong, N. B.; Lee, S. T.; Xie, S. S. *Adv. Mater.* **2000**, *12*, 1186.
(28) Vyshnyakova, K. L.; Pereselentseva, L. N.; Cambaz, Z. G.; Yushin, G. N.; Gogotsi, Y. *Br. Ceram. Trans.* **2004**, *103*, 193.
(29) Liang, C. H.; Meng, G. W.; Zhang, L. D.; Wu, Y. C.; Cui, Z. *Chem. Phys. Lett.* **2000**, *329*, 323.
(30) Deng, S. Z.; Wu, Z. S.; Zhou, J.; Xu, N. S.; Chen, J.; Chen, J. *Chem. Phys. Lett.* **2002**, *356*, 511.
(31) Dai, H.; Wang, E. W.; Lu, Y. Z.; Fan, S. S.; Lieber, C. M. *Nature (London)* **1995**, *375*, 769.
(32) Kharlamov, A. I.; Loichenko, S. V.; Kirillova, N. V.; Fomenko, V. V.; Bondarenko, M. E.; Zaitseva, Z. A. *Inorg. Mater.* **2003**, *39* (3), 260.
(33) Yang, Z. X.; Xia, Y. D.; Mokaya, R. *Chem. Mater.* **2004**, *16*, 3877.
(34) Ye, H.; Titchenal, N.; Gogotsi, Y.; Ko, F. *Adv. Mater.* **2005**, *17*, 1531.
(35) We, J.; Li, K. Z.; Li, H. J.; Fu, Q. G.; Zhang, L. *Mater. Chem. Phys.* **2006**, *95*, 140.
(36) Li, Z. J.; Li, H. J.; Chen, X. L.; Meng, A. L.; Li, K. Z.; Xu, Y. P.; Dai, L. *Appl. Phys. A* **2003**, *76*, 637.
(37) Li, H. J.; Li, Z. J.; Meng, A. L.; Li, K. Z.; Zhang, X. N.; Xu, X. P. *J. Alloys Compd.* **2003**, *352*, 279.
(38) Bogart, T. E.; Dey, S.; Lew, K.-K.; Mohney, S. E.; Redwing, J. M. *Adv. Mater.* **2005**, *17*, 114.
(39) Sander, M. S.; Prieto, A. L.; Gronsky, R.; Sands, T.; Stacy, A. M. *Adv. Mater.* **2002**, *14*, 665.
(40) Olego, D.; Cardona, M. *Phys. Rev. B* **1982**, *25*, 3889.
(41) Feng, Z. C.; Mascarenhas, A. J.; Choyke, W. J.; Powell, J. A. *J. Appl. Phys.* **1998**, *64*, 3176.
(42) Shen, G. Z.; Chen, D.; Tang, K. B.; Qian, Y. T.; Zhang, S. Y. *Chem. Phys. Lett.* **2003**, *375*, 177.
(43) Han, W. Q.; Fan, S. S.; Li, Q. Q.; Liang, W. J.; Gu, B. L.; Yu, D. P. *Chem. Phys. Lett.* **1997**, *265*, 374.
(44) Hu, J. Q.; Lu, Q. Y.; Tang, K. B.; Deng, B.; Jiang, R. R.; Qian, Y. T.; Yu, W. C.; Zhou, G. E.; Liu, X. M.; Wu, J. X. *J. Phys. Chem. B* **2000**, *104*, 5251.
(45) Shim, H. W.; Kim, K. C.; Seo, Y. H.; Nahm, K. S.; Suh, E.-K.; Lee, H. J.; Hwang, Y. G. *Appl. Phys. Lett.* **1997**, *70*, 1757.
(46) Xi, G. C.; Peng, Y. Y.; Wan, S. M.; Li, T. W.; Yu, W. C.; Qian, Y. T. *J. Phys. Chem. B* **2004**, *108*, 20102.
(47) Han, W. Q.; Fan, S. S.; Li, Q. Q.; Hu, Y. D. *Science* **1997**, *277*, 1287.
(48) Yang, W.; Araki, H.; Hu, Q. L.; Ishikawa, N.; Suzuki, H.; Noda, T. *J. Cryst. Growth* **2004**, *264*, 278.